PROCEEDINGS OF SPIE

SPIEDigitalLibrary.org/conference-proceedings-of-spie

Initial investigation of the angular dependence of the NOAA-20 VIIRS solar diffuser BRDF change factor

Ning Lei, Xiaoxiong Xiong

Ning Lei, Xiaoxiong Xiong, "Initial investigation of the angular dependence of the NOAA-20 VIIRS solar diffuser BRDF change factor," Proc. SPIE 10781, Earth Observing Missions and Sensors: Development, Implementation, and Characterization V, 1078116 (23 October 2018); doi: 10.1117/12.2324530

SPIE.

Event: SPIE Asia-Pacific Remote Sensing, 2018, Honolulu, Hawaii, United States

Initial Investigation of the Angular Dependence of the NOAA-20 VIIRS Solar Diffuser BRDF Change Factor

Ning Lei*[a] and Xiaoxiong Xiong[b]

[a]Science Systems and Applications, Inc., 10210 Greenbelt Road, Suite 600, Lanham, MD 20706 USA
[b]Sciences and Exploration Directorate, NASA Goddard Space Flight Center, Greenbelt, MD 20771 USA

* **Corresponding author:** ning.lei@ssaihq.com, tel: +1-301-867-2066

ABSTRACT

The NOAA-20 (formerly the Joint Polar Satellite System-1) satellite was launched on November 18, 2017. One of the five scientific instruments aboard the NOAA-20 satellite (N20) is the Visible Infrared Imaging Radiometer Suite (VIIRS). The VIIRS scans the earth surface in 22 spectral bands, of which 14 are denoted as the reflective solar bands (RSBs) with design band central wavelengths from 412 to 2250 nm. The VIIRS regularly performs on-orbit radiometric calibration of its RSBs, primarily through observations of an onboard sunlit solar diffuser (SD). The on-orbit change of the SD bidirectional reflectance distribution function (BRDF) value, denoted as the H-factor, is determined by an onboard solar diffuser stability monitor (SDSM). We have shown that the H-factor for the SD on the VIIRS instrument on the Suomi National Polar-orbiting Partnership (SNPP) satellite is both incident and outgoing sunlight direction dependent. This angular dependence profoundly affects the on-orbit radiometric calibration process and results. Here, we give preliminary results for the angular dependence for the N20 VIIRS SD H-factor, and compare the dependence with that for the SNPP VIIRS.

Index Terms: N20 VIIRS, radiometric calibration, solar diffuser, BRDF, H-factor, angular dependence

1. INTRODUCTION

The Visible Infrared Imaging Radiometer Suite (VIIRS) instrument is a passive earth observing scanning sensor. Fourteen of the 22 spectral bands are denoted as the reflective solar bands (RSBs) with design band central wavelengths from 412 to 2250 nm. The RSBs, by design, are radiometrically calibrated on-orbit primarily by observing the onboard sunlit solar diffuser (SD)[1]. The second VIIRS is on the NOAA-20 (N20) satellite launched on November 18, 2017. The N20 satellite has the same equator crossing time of 13:30±10 min as the Suomi National Polar-orbiting Partnership (SNPP) satellite on which the first VIIRS instrument resides, and has the same nominal orbital time period of 101.5 min.

Fig. 1 illustrates the physical components related to the on-orbit RSB calibration. The sunlight goes through the SD screen and then is diffusely scattered by the SD to provide a radiance source. The spectral radiance of the SD scattered sunlight is proportional to the SD BRDF at the mission start and the change factor of the BRDF since launch. The on-orbit BRDF change factor, commonly denoted as the H-factor, is determined by the onboard solar diffuser stability monitor (SDSM)[1].

Earth Observing Missions and Sensors: Development, Implementation, and Characterization V
edited by Xiaoxiong Xiong, Toshiyoshi Kimura, Proc. of SPIE Vol. 10781, 1078116

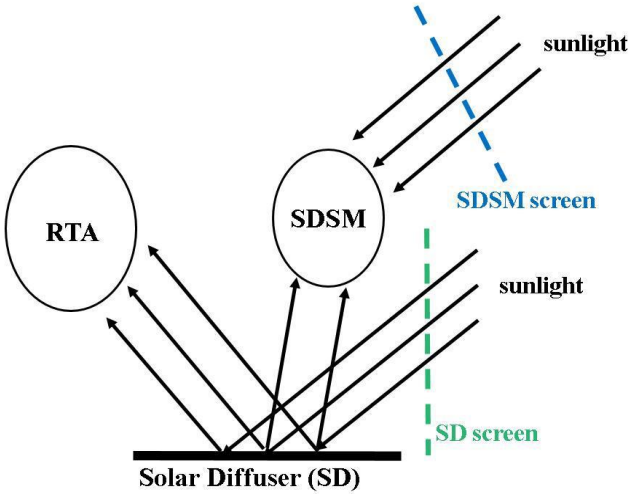

Figure 1. A sketch that shows the components related to the VIIRS on-orbit radiometric calibration. The SDSM and the SD screens are otherwise opaque plates with through holes. The RTA stands for the rotating telescope assembly that directs incoming light to the detector focal planes.

When in operation, the eight SDSM detectors, with design band central wavelengths from 412 to 926 nm, receive photons from the Sun through an attenuation screen denoted as the SDSM screen and the SD reflected sunlight almost at the same time. The ratio of the SDSM signal strengths adjusted for the SD and the SDSM screen transmittance and the sun-sensor distance is a direct measure of the H-factor.

However, the H-factor directly measured by the SDSM is along the SD-to-SDSM direction and what we need is the H-factor along the SD-to-RTA direction. It has been discovered that the H-factor for the first VIIRS instrument onboard the SNPP satellite[2-3] is angle dependent. Here we determine whether the H-factor for the second VIIRS is angle dependent.

2. METHODOLOGY

To determine whether the H-factor is angle dependent, we use the SDSM SD observations, as we did for the SNPP VIIRS[2,4]. As shown in Fig. 2, for the two points 1 and 2, if the solar angles are the same, the ratio of the digital counts from the SD view cancels the SD screen transmittance and the BRDF at the mission start to yield

$$\frac{\mathrm{SR}(t_2)\mathrm{H}_{\mathrm{SDSM}}(t_2,\vec{\phi}(t_1))}{\mathrm{SR}(t_1)\mathrm{H}_{\mathrm{SDSM}}(t_1,\vec{\phi}(t_1))} = \frac{dc_{\mathrm{SD,p}}(t_2,\vec{\phi}(t_1))}{dc_{\mathrm{SD}}(t_1,\vec{\phi}(t_1))} \quad , \tag{1}$$

where the SR is the spectral response function for an SDSM detector, $\vec{\phi}$ is the solar angle, and dc_{SD} represents the digital count with background subtracted from the SD view. In equation (1), we use $\mathrm{H}_{\mathrm{SDSM}}$ to indicate the H-factor along the SD-to-SDSM direction. We use $dc_{\mathrm{SD,p}}$ to indicate the digital count at time t_2 with the solar angle at time t_1. In general, it is impossible to have a digital count that happens at a later time t_2 and at the exact solar angle for an early time t_1. Hence we use a subscript "p" to indicate that the digital count at the later time is a pseudo-digital count that must be constructed through interpolations of measured values. Equation (1) assumes that the spectral response function is sharp enough in the wavelength space to be regarded as a Dirac delta function. The advantage in using equation (1) is the removal of the SD screen transmission function that may not be exactly known. Additionally, equation (1) uses the property that the H-factor at the early mission is very close to one and thus is not particularly angle dependent. Note that the small angular dependence at an early mission time can be taken into account as we did for the SNPP VIIRS[4].

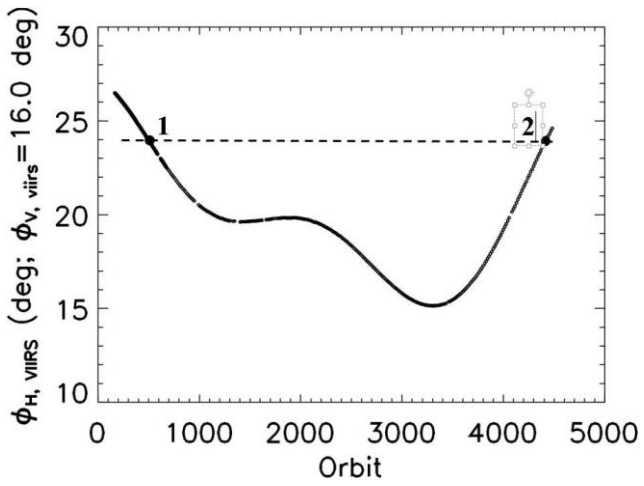

Figure 2. Circles indicate the solar angles in the VIIRS coordinate system when the SDSM sees the sunlit SD. The VIIRS coordinate system is such defined so that the z axis is along the RTA to the center of the earth view port and the x axis is along the normal of the SD screen. The solar azimuth angle $\phi_{\mathrm{H,VIIRS}}$ is defined as the negative of the angle that the solar vector projected onto the xy plane makes with the x axis, and the solar declination angle $\phi_{\mathrm{V,VIIRS}}$ is defined as the angle that the solar vector projected onto the xz plane makes with the x axis.

To find $dc_{\mathrm{SD,p}}(t_2, \vec{\phi}(t_1))$, we rely on the fact that

$$dc_{\mathrm{SD,p}}\left(t, \vec{\phi}(t)\right) = dc_{\mathrm{SD}}\left(t, \vec{\phi}(t)\right). \tag{2}$$

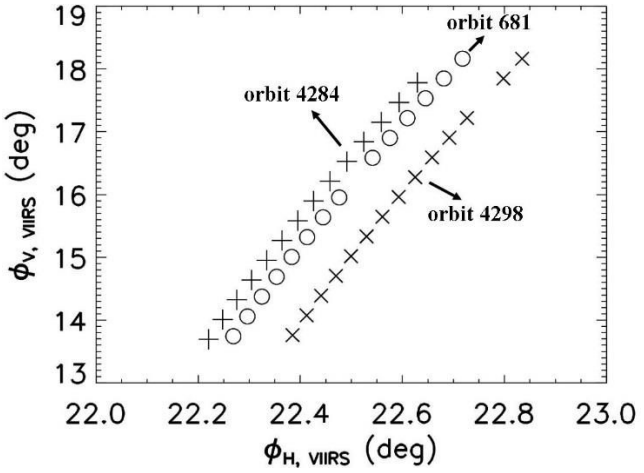

Figure 3. Circles, pluses, and crosses are for the solar angles in the VIIRS coordinate system when the SDSM sees the sunlit SD at orbits 681, 4284, and 4298, respectively.

We select t_1 as satellite orbit 681. Note that the nominal satellite orbit time period is 101.5 min. To find a t_2 and $dc_{\mathrm{SD,p}}(t_2, \vec{\phi}(t_1))$, we examine the solar angles shown in Fig. 3. The figure shows that the solar angles at orbit 681 are in between those at orbits 4284 and 4298. As a result, we can use $dc_{\mathrm{SD}}\left(t_3, \vec{\phi}(t_3)\right)$ and $dc_{\mathrm{SD}}\left(t_4, \vec{\phi}(t_4)\right)$ to calculate $dc_{\mathrm{SD,p}}(t_2, \vec{\phi}(t_1))$ where, t_3 and t_4 are respective times on orbits 4284 and 4298. We define $\vec{\phi}(t_3)$ and $\vec{\phi}(t_4)$ to have the

same solar declination angle as $\phi_{\mathrm{V,VIIRS}}(t_1)$ and $\phi_{\mathrm{H,VIIRS}}(t_3) \le \phi_{\mathrm{H,VIIRS}}(t_1) \le \phi_{\mathrm{H,VIIRS}}(t_4)$. Fig. 3 reveals that the solar angular curve for orbit 681 is parallel to those of orbits 4284 and 4298 and thus presents a simpler case[4] since we can set

$$t_2 = t_3 + \frac{t_4 - t_3}{\phi_{\mathrm{H,VIIRS}}(t_4) - \phi_{\mathrm{H,VIIRS}}(t_3)} \times (\phi_{\mathrm{H,VIIRS}}(t_1) - \phi_{\mathrm{H,VIIRS}}(t_3)) \quad (3)$$

to obtain

$$dc_{\mathrm{SD,p}}\left(t_2, \vec{\phi}(t_1)\right) = \frac{(t_4 - t_2) \times dc_{\mathrm{SD}}\left(t_3, \vec{\phi}(t_3)\right) + (t_2 - t_3) \times dc_{\mathrm{SD}}\left(t_4, \vec{\phi}(t_4)\right)}{t_4 - t_3} \ . \quad (4)$$

We calculate the ratio of the SDSM detector response functions in equation (1) from the sun view data through

$$dc_{\mathrm{Sun}}\left(t, \vec{\phi}(t)\right) = \tau^{\mathrm{eff}}_{\mathrm{SDSM}}(\vec{\phi}(t)) \times \mathrm{SR}(t)\mathrm{E}_{\mathrm{sun}}(\lambda_d, t) \ , \quad (5)$$

where t indicates a time on a particular orbit, $\tau^{\mathrm{eff}}_{\mathrm{SDSM}}$ is the effective SDSM screen transmittance refined with both the yaw maneuver and regular on-orbit SDSM data[5], λ_d indicates band central wavelength for SDSM detector d, and $\mathrm{E}_{\mathrm{sun}}$ is the solar spectral irradiance at the VIIRS.

3. RESULTS

Assuming $\mathrm{H}_{\mathrm{SDSM}}$ at t_1 is not solar angle dependent since t_1 is early in the mission, we use equation (1) to calculate $\mathrm{H}_{\mathrm{SDSM}}$ at t_2 that is determined by equation (3) to be about orbit 4288. To give an example, in Fig. 4 we plot the $\mathrm{H}_{\mathrm{SDSM}}$ at t_2 for SDSM detector 1. The obtained $\mathrm{H}_{\mathrm{SDSM}}$, indicated as the circles, follows a linear function of the solar angle $\phi_{\mathrm{V,SD}}$ defined

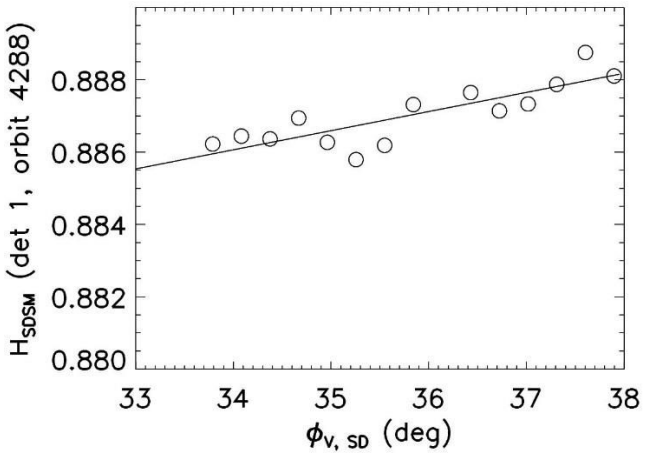

Figure 4. Circles indicate $\mathrm{H}_{\mathrm{SDSM}}$ at t_2 calculated by using equation (1), versus $\phi_{\mathrm{V,SD}}$ for SDSM detector 1 with t_2 =orbit 4288, where $\phi_{\mathrm{V,SD}}$ is the angle between the incident sunlight and the SD surface. The solid line indicates the best fit of a linear polynomial of $\phi_{\mathrm{V,SD}}$ to the measured $\mathrm{H}_{\mathrm{SDSM}}$.

as the angle between the sunlight and the SD surface. The slope of the linear function is 0.00053 deg^{-1}. We calculate the $\mathrm{H}_{\mathrm{SDSM}}$ at t_2 for all eight SDSM detectors and plot the slopes versus 1- $\mathrm{H}_{\mathrm{SDSM}}$ at $\phi_{\mathrm{V,SD}} = 35.5$ deg in the left chart of Fig. 5. To compare, we also plot the slopes for the SNPP VIIRS versus 1- $\mathrm{H}_{\mathrm{SDSM}}$ in the right chart[4] of Fig. 5. Fig. 5 reveals that at the same 1 – $\mathrm{H}_{\mathrm{SDSM}}$, both SDs on the N20 and SNPP VIIRS instruments yield about the same amount of solar angular dependence at least along the solar angles of satellite orbits.

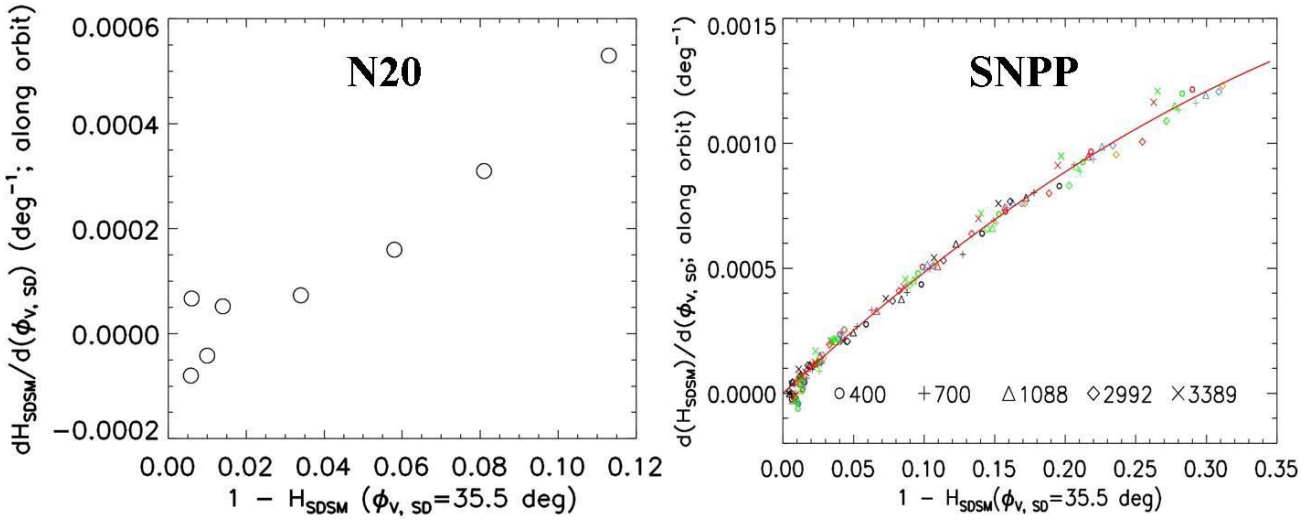

Figure 5. $dH_{SDSM}/d\phi_{V,SD}$ along the solar angles of satellite orbits at $\phi_{V,SD} = 35.5$ deg. (Left) for the N20 VIIRS and (right) for the SNPP VIIRS.

4. AN APPLICATION OF THE H-FACTOR ANGULAR DEPENDENCE

In the last section, we showed that the amounts of the solar angular dependence of the N20 and SNPP VIIRS SD H_{SDSM} along the satellite orbits are about the same at the same H_{SDSM}. Since both the SNPP and N20 satellites orbit the Earth in the same plane, the nearly same amount of solar angular dependence at the same H_{SDSM} for both the SDs indicates that the SNPP VIIRS SD H-factor angular dependence may be valid to the N20 VIIRS SD H-factor.

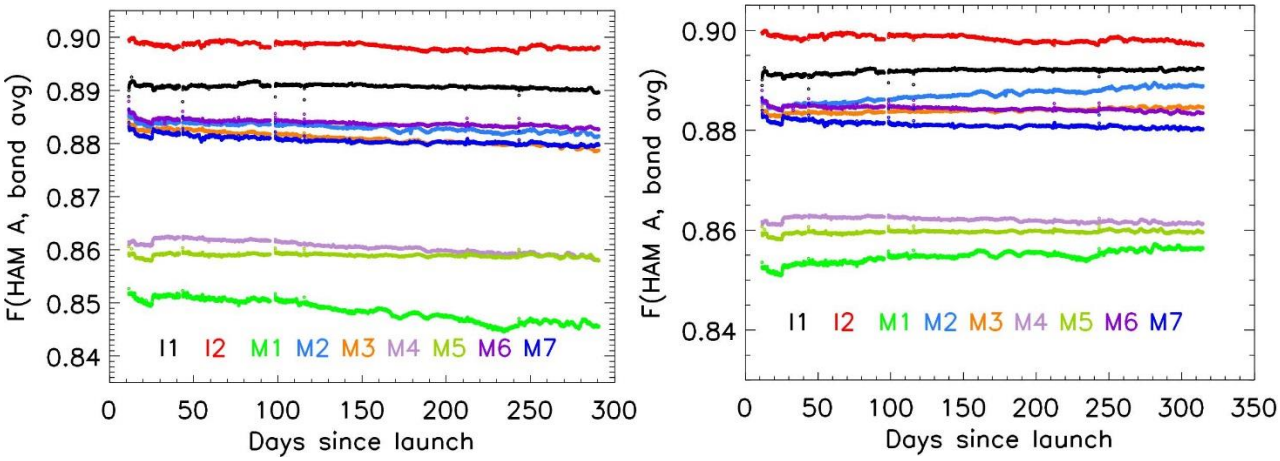

Figure 6. The SNPP VIIRS VISNIR band F-factors calculated from (left) the measured H_{SDSM} and (right) from the H_{RTA} that is determined through equation (6) with the RSR de-convoluted H_{SDSM}. The F-factors are averaged over all the detectors in a band and are for half-angle-mirror side A, and high-gain stage for dual-gain bands.

For the SNPP VIIRS, we have[6]

$$H_{RTA} = H_{SDSM} \times \frac{1+\alpha_{RTA}(\lambda)*(1-H_{SDSM})}{1+\alpha_{H}(\lambda)*(1-H_{SDSM})*\left(\phi_{H,SD}-\phi_{H0}\right)}, \quad (6)$$

where ϕ_{H0}=48.0 deg, $\phi_{H,SD}$ is the solar azimuth angle in the SD plane[6]. In equation (6)

$$\alpha_{H}(\lambda) = 0.0033 \times (1 - \frac{0.076}{\lambda^{2.48}}), \quad (7)$$

where λ is the band central wavelength in microns[6] and $\alpha_{RTA}(\lambda)$ is obtained from matching the lunar F-factor with the SD F-factor calculated with the SNPP H_{SDSM}, where the F-factor is a correction factor to the initially calculated scene spectral radiance[1]. Fig. 6 shows the N20 VIIRS visible near infrared (VISNIR) band F-factors using H_{SDSM} (left) and H_{RTA} (right). In generating the right chart of Fig. 6, we have de-convoluted the measured N20 H_{SDSM}[7], using the SNPP VIIRS SDSM detector RSRs as approximations. The F-factors calculated with the H_{RTA} show that since launch the F-factor moves up about 0.5% for the M1 band, 0.3% for the M2 band, 0.2% for the M3 band, stays nearly flat for the M4, I1, and M5 bands, and decreases about 0.2% for the I2 and M7 bands.

5. SUMMARY

We have obtained the initial solar declination angular dependence of the measured H_{SDSM} at day 302 after launch (orbit number 4288) along the solar angles on satellite orbit 681 (day 48). As for the SNPP VIIRS, the dependence is stronger at a shorter wavelength. At the wavelength of the SDSM detector 1 with the design wavelength of 412 nm that is the shortest among the 8 SDSM detectors, the derivative of the H_{SDSM} over the solar declination angle along the satellite orbit has a value of 0.00053 deg^{-1}. Very importantly, we have found that at the same H_{SDSM}, the dependence has nearly the same amount as the SNPP VIIRS. Since the SNPP and N20 share the same orbital plane, the finding indicates that the H-factor angular dependence for the N20 VIIRS may be the same as that for the SNPP VIIRS. Applying the SNPP VIIRS H-factor angular dependence for the N20 VIIRS, we have obtained the N20 VIIRS H_{RTA} from the RSR de-convoluted H_{SDSM} and applied the H_{RTA} to calculate the F-factors.

ACKNOWLEDGMENTS

We thank Kevin Twedt of Science Systems and Applications, Inc. (SSAI), Lanham, MD, USA, for many useful comments.

REFERENCES

1. Joint Polar Satellite System (JPSS) VIIRS Radiometric Calibration Algorithm Theoretical Basis Document (ATBD); NASA Goddard Space Flight Center: Greenbelt, MD, USA, 2013.

2. N. Lei, K. Chiang, and X. Xiong, "Examination of the angular dependence of the SNPP VIIRS solar diffuser BRDF degradation factor", *Proc. SPIE*, vol. 9218, paper ID: 9218-1N, 2014.

3. J. Sun and M. Wang, "Visible Infrared Imaging Radiometer Suite solar diffuser calibration and its challenges using a solar diffuser stability monitor", Applied Optics, vol. 53, pp. 8571-8584, 2014, DOI: 10.1364/AO.53.008571.

4. N. Lei and X. Xiong, "Products of the SNPP VIIRS SD Screen Transmittance and the SD BRDFs from Both Yaw Maneuver and Regular On-orbit Data", *IEEE Trans. Geosci. Remote Sens.* vol. 55(4), pp. 1975-1987, 2017; DOI: 10.1109/TGRS.2016.2633967.

5. N. Lei and X. Xiong, "Initial determination of the screen transmittance for the NOAA-20 VIIRS with both yaw maneuver and regular on-orbit data", *Proc. SPIE*, vol. 10781, paper ID: 10781-16, 2018.

6. N. Lei and X. Xiong, "Impacts of the Angular Dependence of the Solar Diffuser BRDF Degradation Factor on the SNPP VIIRS Reflective Solar Band On-Orbit Radiometric Calibration", *IEEE Trans. Geosci. Remote Sens.* vol. 55(3), pp. 1537-1543, 2017, DOI: 10.1109/TGRS.2016.2626963.

7. N. Lei, Z. Wang, J. Fulbright, and X. Xiong, "Effect of the SDSM detector relative spectral response in determining the degradation coefficient of the SNPP VIIRS Solar Diffuser reflectance", *Proc. SPIE*, Vol. 8866, Paper ID: 8866-1I, 2013.